Ultrasonic monitoring of barrel wear and screw status

Jen, C.-K.; Sun, Z.; Kobayashi, M.

Publisher's version / Version de l'éditeur:

Measurement Science & Technology, 16, 2005-03-01

Ultrasonic Monitoring of Barrel Wear and Screw Status

C.-K. Jen[+*], Z. Sun[+], and M. Kobayashi[#]

[+] Industrial Materials Institute, National Research Council of Canada
Boucherville, Quebec, Canada J4B 6Y4.
[#] Department of Electrical and Computer Engineering, McGill University
Montreal, Quebec, Canada H3A 2A7

Abstract

Ultrasonic sensors together with a fast data acquisition system have been used to measure barrel wear, screw wear, screw misalignment, and screw deflection during low-density polyethylene as well as high-density polyethylene extrusion on a Werner & Pfleiderer 30 mm twin-screw extruder. The sensors include sol-gel sprayed high temperature (HT) piezoelectric thick ceramic film ultrasonic transducers (UTs), stand-alone HTUTs, and air-cooled buffer rod type sensors consisting of a room temperature UT and a non-clad or clad buffer rod to which the room temperature UT is attached. The installation and use of these sensors are non-intrusive to the extruder and non-destructive to the polymers being processed. This study has demonstrated the capability of ultrasonic sensors for real-time monitoring of barrel wear and screw status at the pumping, mixing and melting zones of extruders via barrel or flange. The merits and limitations of these sensors are presented. The measurement speed and accuracy are discussed.

[*] Corresponding author. Tel: 450-641-5085, Email:cheng-kuei.jen@cnrc-nrc.gc.ca

1. Introduction

The conditions of barrel and screw are important to polymer extrusion processes. [1,2,3]. The presence of barrel and screw wear, screw misalignment and deflection can affect adversely the product quality or reduce the productivity. One industrial attitude is to live with them. In order to compensate for the reduced output, one can raise up the melt temperature to a higher than desired level or increase the screw rotation speed, and this often results in the deterioration of the product quality on top of the production efficiency reduction.

The wear may come from abrasion by abrasive materials such as glass-fiber reinforced polymers, chemical corrosion resulted from, for example, degradation of PVC releasing hydrogen chloride, and erosion, etc. Commonly the wear occurs in the transition zone where it is limited to a short length of the barrel and screw or in the metering zone, where a considerable length of barrel and screw may be affected. In the latter the degree of the wear tapers off toward the feed end. During extrusion, the position of the central axis of a screw shaft could constantly change. This constant variation can be caused by the misalignment of the screw, as well as the un-even resultant force exerted on the long axle of the screw coming from screw weight, asymmetric melt load and pressure in the cross-section of the screw shaft, and asymmetric friction between the screw and the viscous material. In this paper, we use the terms “misalignment” and “deflection” to define the behavior of a screw. By screw misalignment, we mean any deviation of the mean position (i.e., average over a long enough process time) of the screw shaft axis from the bore axis of the extruder channel. By screw deflection, we mean the transient deviation of the screw shaft from its mean position. Since the clearance between the screw flight and barrel wall is small, the screw misalignment and deflection could cause metal-metal contact between the barrel and screw, and this may result in serious barrel and screw wear or even damage to the gear box.

It is well known that extrusion is the basic unit for many other polymer processes including injection molding and blow molding. A common technique for wear inspection is to firstly shut down the extruder, take out and clean the screws, and then perform off-line mechanical measurements on individual screw and barrel elements. Such an approach is accurate but may induce significant production loss in particular for large extruders. Furthermore, this off-line measurement is not able to provide information on screw misalignment and deflection.

Given the high production rates on some of the production lines (up to tens of tons/hour at the current technology stage) and the long shutdown time (in the order of days or week) required for manual screw and barrel check-up, a technology capable of in-line monitoring of screw and barrel statuses would result in significant savings by avoiding costly unnecessary shutdowns or by providing preventive warning on the screw and barrel status before the malfunctioning of the screw has deteriorated the product quality or before any damage has been made to the costly gear box.

In this paper, we will report the use of four types of ultrasonic sensors for in-line monitoring of both the barrel wear and screw wear, and screw misalignment and deflection during extrusion. The sensors are (1) sol-gel sprayed high temperature (HT) piezoelectric thick ceramic film ultrasonic transducers (UTs), (2) stand-alone HTUTs, (3)

air-cooled non-clad buffer rod type sensors consisting of a room temperature UT and a non-clad buffer rod to which the room temperature UT is attached, and (4) air-cooled clad buffer rod type sensors consisting of a room temperature UT and a clad buffer rod to which the room temperature UT is attached. The installation and use of these sensors are non-intrusive to the extruder and non-destructive to the polymers being processed. Experimental data obtained during extrusion of low-density polyethylene (LDPE) and high-density polyethylene (HDPE) on a Werner & Pfleiderer (W&P) 30-mm twin-screw extruder will be presented.

2. Wear Measurement Principle and Data Acquisition System

Ultrasonic techniques have been reported as on-line methods to monitor the polymer extrusion processes [4-7]. A major characteristic of ultrasound is that it can propagate in the barrel and molten polymers without much loss in its energy. When there are property changes in the melt, the ultrasonic characteristics such as reflection coefficient at the interface between the barrel wall and the melt, and the ultrasonic velocity and attenuation in the melt will change. In addition, the ultrasonic energy will be scattered, e.g., by the fillers or unmelted pellets in the melt. This means that the variation of reflection coefficient, velocity, attenuation and scattered energy of the ultrasound propagating in the molten polymer may be used to characterize the melt properties such as viscosity, filler concentration, degradation, melting and mixing conditions, dispersion, residence time distribution, etc [4-7]. When propagating inside a barrel, the traveling time for ultrasound to propagate from the external to internal barrel surfaces allow for barrel thickness measurement.

A schematic diagram for the ultrasonic wave propagation in a pulse/echo mode is given in Fig. 1. The ultrasonic longitudinal waves generated by a UT mounted on the external surface of the barrel propagate into the barrel to its barrel inner wall contacting the melt. By this arrangement, the technique is non-intrusive to the barrel and the cavity. The ultrasonic energy, which is on average of only tens of milliwatts and thus considered as non-destructive to polymers, is then partly reflected at the barrel inner wall/molten polymer interface (echo denoted by L^1 in Fig. 1), and partly transmitted to the molten polymer then reflected either by the flight (echo denoted by L_{2F}) or the root (echo denoted by L_{2R}) of the rotating screw. The echoes L^2, L^3, L_{4F}, L_{6F}, L_{4R} and L_{6R}, represent the further round trip echoes in the corresponding media. The same UT receives the returned echoes.

The echoes L^1, L^2 and L^3 in Fig. 1 represent the first, second and third round trip echoes, respectively, inside the extrusion barrel. The barrel wear δd_B, which is the reduction of the thickness of the barrel wall d_B with respect to that of an un-worn one, can be measured as

$$\delta d_B = d_{B0} - d_B = d_{B0} - v_{LB} * t_B/2, \qquad (1)$$

where d_{B0} is the nominal barrel thickness, v_{LB} is the ultrasonic longitudinal velocity in the barrel, and t_B is the time delay between the two echoes L^1 and L^2 (or echoes L^2 and L^3).

In Fig. 1 the signals L_{2F}, L_{4F} and L_{6F} are respectively the first, second and third round trip echoes off the flight of the screw, and the signal L_{2R}, L_{4R} and L_{6R} the first,

second and third round trip echoes, respectively off the root of the screw. Because the wear is commonly severer at the flight than at the root, in this investigation, we only consider the screw wear and use only echoes L_{2F}, L_{4F} or L_{6F} for wear measurement and not echoes L_{2R}, L_{4R} and L_{6R}. The distance, d_F, between the barrel wall and screw flight can be expressed as a function of the nominal barrel/screw clearance d_{F0}, screw wear δd_F_screw, degree of screw misalignment δd_F_malgn, screw deflection δd_F_defl, and barrel wear δd_B:

$$d_F = d_{F0} + \delta d_F\_screw + \delta d_F\_malgn + \delta d_F\_defl + \delta d_B , \quad (2)$$

where δd_F_malgn and δd_F_defl can have either positive or negative values depending on whether the misalignment and deflection makes the screw farther or closer to the sensor in comparison with the case where no misalignment and deflection are present, and all other parameters carry positive values. In the above equation, d_{F0} is usually known, and d_F can be measured as $d_F = v_{LP}*t_P/2$ with v_{LP} being the ultrasonic velocity in the polymer being probed and t_P the time delay between the two echoes L_{2F} and L_{4F} (or L^1 and L_{2F} or echoes L_{4F} and L_{6F}).

On the right-hand side of Eq. (2), every item can be considered as constant at the probed location and during a short observation period except δd_F_defl which represents the transient deviation of screw shaft from its average position. Thus any transient change of d_F on the left-hand side of equation is caused by the variation of δd_F_defl. In other words, the screw deflection can be determined from the fluctuation of d_F. As will be seen later in the paper, the fluctuation of d_F, hence the screw deflection, is measurable.

By taking the average of Eq. (2) over a long enough process time and taking into account that the average of δd_F_defl is zero, we have

$$\langle d_F \rangle = d_{F0} + \delta d_F\_screw + \delta d_F\_malgn + \delta d_B , \quad (3)$$

where $\langle \cdot \rangle$ represents the average over a certain observation time. As can be seen clearly in Eq. (3), in the case where the barrel wall is not worn and screw misalignment is absent, the screw wear δd_F_screw can readily be measured as

$$\delta d_F\_screw = \langle d_F \rangle - d_{F0} = v_{LP}*\langle t_P \rangle/2 - d_{F0}. \quad (4)$$

In the case where the barrel wall is worn but there is no screw misalignment, the screw wear can be determined as

$$\delta d_F\_screw = \langle d_F \rangle - d_{F0} - \delta d_B = v_{LP}*\langle t_P \rangle/2 + v_{LB}*t_B/2 - d_{F0} - d_{B0}. \quad (5)$$

In the case where the screw is misaligned, installation and use of multiple sensors at different sections along the extruder barrel may be required to determine the screw misalignment and the screw wear will be determined as

$$\delta d_F\_screw = \langle d_F \rangle - d_{F0} - \delta d_F\_malgn - \delta d_B . \quad (6)$$

In practical situations, the product quality and production efficiency can be mostly affected by the combined effect of screw wear, barrel wear, and screw misalignment, i.e., the barrel/screw clearance, in addition to screw deflection. In other words, the barrel/screw clearance and screw deflection can provide valuable information about the health of the process and the extruder without the need of identifying each individual

contributing factor to the barrel/screw clearance change. In the following section, we will present implementations of various sensors for barrel wear, barrel/screw clearance, and screw deflection measurements. By performing the measurements at several sections along the extruder barrel, the screw wear can be measured through Eq. (6).

All ultrasonic signals are acquired with a PC based data acquisition system. In order to determine the ultrasonic time delay t_P in the molten polymer during extrusion whereby d_F is measured through $d_F = v_{LP}*t_P/2$, it is required that at each sensor location the ultrasonic echo signals reflected from the very same area of the screw flight be measured during screw rotation. Because of the odd shape and the rotation of the screw, it has been found necessary to acquire data at high repetition rate such that the angular position of the screw could be tracked during extrusion and that the measurements could be taken for nearly the same relative sensor-screw position. To meet this need, a GAGE A/D board with 12-bit resolution and 8 Mega-sample on-board memory was installed. Using the multiple-recording mode of this board and our current ultrasonic sensors and software, we could acquire up to 2000 signals of 2000 sample points within one second for two channels. At an acquisition speed of 2000 signals per second, if the screw rotates at 200 RPM, we will have 600 signals per rotation, which corresponds to an angular resolution of 0.6 degree.

3. Sensors and Measurements

In this section different sensors are used at different zones such as pumping, mixing and melting. The distinct features of each sensor will be mentioned. Each sensor was installed in such a way that its beam axis was directed perpendicularly to the screw shaft to be monitored. We will use the signals L^1 and L^2, as well as L_{2F}, L_{4F}, and/or L_{6F} to demonstrate that these sensors can measure the barrel wall thickness d_B and the clearance d_F between the barrel wall and the screw flight tip. The measurement accuracy will be discussed in the next section.

3.1 Sol-Gel Sprayed HTUT at the Pumping Zone

Thick piezoelectric lead-zircontate-titanate (PZT) films have been demonstrated as efficient UTs in [8]. In [9] a sol-gel spray technique using the fine lithium titanate or PZT powders dispersed into PZT solution has been applied to fabricate HTUTs operational at temperatures up to 250°C. In the present work, the ball-milled bismuth titanate (BIT) fine powders are dispersed into lead-zirconate-titanate (PZT) solution to form the gel. BIT is used because its Curie temperature is 675°C and it can operate at temperatures up to 600°C or higher [10]. The gel is then sprayed onto the top surface of an extruder adaptor at a room temperature. The adaptor has been chosen here for demonstration purpose. The films with desired thickness of 90 μm have been obtained through a multilayer coating approach. Piezoelectricity is achieved using the corona discharge poling method. The area of the top electrode, which is made of silver plate painted onto the barrel adaptor surface, has an optimized diameter of 11mm [10]. The center frequencies of ultrasonic signals generated by these films range between 3.6 and 30 MHz and their bandwidths are more than 2 MHz. The main advantages of such

sensors are that they (1) do not need couplant, (2) can be coated onto curved surfaces and (3) can operate continuously at temperatures up to 600°C or higher [10]. This covers the entire external barrel surface temperature range for most polymer extrusion processes (normally less than 350°C). In order that the drying, firing and annealing of the film deposited on the barrel surface can be carried out, an oven large enough to accommodate the barrel is needed. A challenge this method has to face is that the firing and annealing processes take place at elevated temperatures and this may change the fine metal structure of a nitrided barrel. A possible solution to this problem is to confine the heating to a small surface area of the film by means of inductive or microwave heating.

Figure 2 shows the sol-gel sprayed BIT/PZT film (light color area) deposited onto the top external surface of an extruder adaptor located at the pumping zone. At the center of the adaptor is a temperature/pressure probe used to measure the melt temperature and pressure. Three 11 mm diameter top silver paste electrodes, which define the active area of HTUT, are aligned with the screw shaft underneath. The center electrode generated the results reported in this paper. We used spring-loaded HT electrical contacts to contact the top electrode and the bottom electrode, the latter being the steel adaptor itself. The monitoring was performed on a Werner & Pfleiderer (W&P) 30mm twin-screw extruder. The monitored screw element was a 20/20 RH conveying bushing as shown in Fig. 3. The probed area was at the pumping zone and is indicated in the figure. The extruded material was an HDPE. The barrel temperature and the melt pressure at the monitored area were about 200 ºC and 1000 psi, respectively. Although the measured average barrel temperature was 200°C, the measured temperature at the barrel adaptor surface was 190°C. Three echoes L^1, L^2 and L^3 reflected from the barrel adaptor/molten polymer interface are shown in Fig. 4. The center frequency of these echo signals is around 10 MHz. The L^1 and L^2 signals have a signal to noise-ratio (SNR) of 35 dB and 10 dB, respectively. The SNR is defined as the ratio of the amplitude of a signal such as L^1 and L^2 to that of the surrounding noise. The SNR can strongly affect the measurement accuracy, which will be discussed later in the text.

Figures 5(a) to 5(d) show the evolution of echoes reflected at the adaptor/molten polymer interface (L^1) and off the screw flight (L_{2F}, L_{4F}, and L_{6F}, etc.) at the pumping zone during the first 40 s data acquisition period as indicated by the horizontal axes. The vertical axis represents the time delay of the ultrasonic echoes. Different from Fig. 4 where the amplitudes of the echoes were shown in height, in Fig. 5 the amplitudes of the echoes are represented in gray levels. The higher is the amplitude, the darker the gray level. The letters A and B denote the echoes reflected by the tip of each of the two screw flights of the 20/20 RH conveying bushing shown in Fig. 3 within one revolution. As one can see from the figures, the time delay between the echoes L^1 and L_{2F} varies as the extrusion goes on within this 40 s period. Figures 5(a) shows more or less stable screw rotation whereas figures 5(b), 5(c) and 5(d) indicate significant deflection, in particular at the process time of 8, 13.5, and 39 seconds. Figure 5(d) also shows the gradual change of the screw flight displacement. These figures clearly demonstrate the ability of the sol-gel sprayed HTUT to monitor the barrel/screw clearance and screw deflection. To show the signal quality, a single trace of the echoes is extracted at 0.25s process time from Fig.5(a) and shown in Fig.6. The SNR of echoes L_{2F}, L_{4F}, etc. is not high and this could affect the screw wear measurement accuracy which will be discussed later in the text.

3.2 Stand-alone HTUT at the Pumping Zone

A high temperature (up to 250°C) broadband stand-alone UT from Sigma Transducers Inc. (Kennewick, Washington) was also used for the measurements. The center frequency of the HTUT was 5 MHz. During the measurements this HTUT together with its mechanical holder was placed on the top of an extrusion adaptor identical to the one shown in Fig. 2 and above the screw shaft underneath as illustrated in Fig. 7. Between probing end of this HTUT and the adaptor surface, a thin layer of Corning silicone oil was applied as ultrasonic couplant to facilitate the propagation of ultrasonic energy from the HTUT to the barrel adaptor. In this particular case, the extruded material was an LDPE instead of the HDPE used in all the other experiments presented in the paper. The monitored screw elements were a normal 28/28 RH bushing and a 28/28 RH bushing downsized by 0.69 mm in diameter as shown in Fig.8. The downsized bushing represents a 0.345mm screw wear on the flight but its root was not downsized. During the measurements, both bushings were placed side by side at the pumping zone of the extruder. The extruded material, the barrel temperature and the pressure at the monitored area, which was the pumping zone, were kept the same as those used by the sol-gel fabricated HTUTs. Since the stand-alone UT can be moved from one location to the other, measurements were first carried out at the unworn and then the worn locations. Because of the nearly identical barrel adaptor used, the ultrasonic signals for the barrel wear measurement here were almost identical to those shown in Fig.4 except the center frequency, which was 5 MHz in the present case. The observed ultrasonic signals at the un-worn and worn (0.345 mm) screw locations are shown in Figs. 9(a) and 9(b), respectively. Figures 9(a) and 9(b) clearly indicate that the time delay between the signals L_{2F} and L_{4F} in Fig. 9(b) at the worn (downsized by 0.345 mm) screw side is much larger than that in Fig. 9(a) at the un-worn side, because of the extra traveling time in the molten LDPE. These figures clearly illustrate the ability of the stand-alone HTUT to monitor the screw wear.

Since the high temperature stand-alone UT can be moved along the barrel, together with a high temperature liquid couplant as shown in Fig. 1, in principle, we can map the barrel and screw wear along the barrels provided that the UT has the access to the external surface of the barrels and without any blockage from the heating band, cooling line, or fixture in between the UT and the internal wall of the barrel. The disadvantage of the HT liquid couplant is that it evaporates at elevated temperatures after certain duration of time and needs to be refreshed at times. Nevertheless, this may be acceptable for barrel wear, screw wear, screw misalignment and screw deflection (not shown here) monitoring. An alternative is to use a solid couplant such as thin gold film to replace the liquid one. However, in order to ensure an acceptable ultrasonic coupling between the stand-alone UT and the barrel, the pressure should be larger than 10 N/mm^2, [11] which is not small. Such large force requirement compromises the advantage of stand-alone transducer for mapping the wear. At present, the stand-alone HTUT used here can operate continuously below 200°C and momentarily (< a few seconds) up to 350°C. Stand-alone UTs capable of operating at higher than 200°C for a long time need to be developed. Also Figs. 9(a) and 9(b) reveal that the signal strength and SNR of this stand-alone HTUT needs to be increased.

3.3 Non-clad Buffer Rod Sensor at the Mixing Zone

Besides the HTUTs mentioned above, commercially available high performance room temperature UT can be used together with a cooling system and a non-clad or clad buffer rod [12,13] to perform the in-line monitoring of barrel wear, screw wear, screw misalignment and deflection. Figure 10 shows the schematic diagram. In this section the use of non-clad buffer rods, which are basically fine grain steel rods of low cost, is described.

The ultrasonic longitudinal waves generated by the room temperature UT, which is on the top surface of a non-clad or clad buffer rod, propagate through a room temperature couplant between the UT and the buffer rod into the buffer rod. The ultrasonic energy is then partly reflected at the buffer rod /barrel external surface interface (echo denoted by L^0 in Fig. 10), and partly transmitted into the barrel. The rest of the ultrasonic path is identical to the one described in section 2 and shown in Fig.1. By this arrangement, the technique is non-intrusive and non-destructive to the barrel and the cavity. In Fig.10 the echoes L^0, $L^{0'}$ and $L^{0''}$ represent the first, second and third round trip echoes, respectively, in the buffer rod. The same UT will receive all returned echoes.

Like in the case of the stand-alone HTUT described in section 3.2, a HT couplant must be used between the buffer rod probing end and the external surface of the barrel. Similarly the sensors shown in Fig.10 can be used to map the barrel and screw wear as long as the sensor has the access to the external surface of the barrel and the ultrasonic beam path between the sensor and internal barrel wall surface is clear of any blockage from heating band, cooling line or extruder fixture. Because a room temperature UT is used, a cooling system, which makes the sensor bulky, is required. Reference [12] has reported the criteria to select the diameter and the length of the non-clad buffer rod. The buffer rod materials are also of importance. For this investigation a 50.8 mm long non-clad steel rod of 25.4 mm diameter was used.

Figure 11 shows this non-clad buffer rod sensor mounted at the bottom of a barrel at the mixing zone with the help of a holder. The heating band did not cover the bottom surface of the barrel. The screw type and area under the monitoring of this sensor is shown in Fig.12. The monitored bushings were a 90°x5x28 RH and 45°x5x28 RH kneading blocks. Figure 13 displays the echo signals reflected respectively from the probe/barrel interface (L^0) and the barrel/molten polymer interface (L^1) captured with the setup shown in Fig. 11. From the schematic diagram shown in Fig.10 and Eq. (1), one can see that the barrel wear can be determined through measurement of time delay t_B between the two echoes L^0 and L^1.

Figure 14 shows the evolution of echoes reflected from the barrel internal wall/molten polymer interface L^1 and off the screws (L_{2F}, L_{4F}, etc.) shown in Fig.13 during a 3.5s extrusion time (20s to 23.5s of data requisition time for one run). The letters A, B, C, D, and E denote the echoes reflected from the five different segments of the kneading blocks illustrated in Fig. 12 with the subscripts 1 and 2 representing the contributions from each of the two contributing reflecting surface areas of each of the five denoted segments. Even though the screw shapes are complex as indicated in Fig.12 the non-clad buffer rod sensor could still monitor the screw positions indicated as A, B, C, D and E at the mixing zone. In [14] ultrasound was also proved to be able to detect the

signals reflected off the screws of different types. Noticeably the barrel/screw clearance was different for different screw segments. Due to the similar shapes of segments A, C, and D and similar relative positions of their contributing reflecting surface areas with respect the ultrasonic sensor, the echoes reflected from segments A, C, and D were received by the sensor at almost the same process time. These echoes interfere with each other in such a way that L_{2F}, L_{4F}, and L_{6F} echoes become un-resolvable in time domain without advanced signal processing. To improve spatial resolution, a sensor with a smaller sensing area can be used so that only one bushing segment is probed at a time. A single trace of the echoes is extracted at 20.75s process time from Fig.14 and displayed in Fig.15 to show the signal quality. As the extrusion monitoring proceeds, clearly the barrel/screw clearance d_F can be measured as the time delay between the two echoes L_{2F} and L_{4F} (or L^1 and L_{2F} or echoes L_{4F} and L_{6F}, etc.) is monitored.

3.4 Clad Buffer Rod Sensor at the Mixing Zone

For industrial extruders sometimes a sleeve, as shown in Fig.16, is utilized as an inner wall of the barrel to protect the expensive barrel against abrasion, corrosion, and erosion. For this kind of extruder, the barrel sleeve can be extracted out of the barrel for restoration in a similar way to pulling out a screw from the barrel. The sleeve temperature is usually measured with a thermocouple introduced to the sleeve through an access hole. In our investigation, we assumed that the access hole had the shape of the Dynisco thermocouple with a largest diameter of 12.7 mm, therefore a clad buffer rod having the same external shape was used here. Our purpose was to demonstrate that this type of clad buffer rod sensor could be used to measure the barrel sleeve wear and the status of the screw. The mixing zone was chosen for the experiments. By comparing the schematic diagram shown in Fig. 10 with that shown in Fig.16 one can realize that the measurement principle explained in section 3.3 can be directly applied here except that the barrel sleeve thickness was measured instead of the barrel wall thickness. Figure 17 shows a clad buffer rod sensor (having the external shape of a Dynisco thermocouple) mounted at the bottom of a barrel at the mixing zone with the help of a holder. In this case the barrel was considered as a simulated barrel 'sleeve'. Air cooling was used. The heating band did not cover the bottom surface of the barrel. A detailed description of the clad buffer rod and its performance can be found in [13]. The clad buffer rod has higher ultrasonic performance than the non-clad buffer rod. It is rugged and not expensive. It is noted that for the measurement configuration given in Fig. 16, a layer of HT couplant was applied between the probing end of the clad buffer rod sensor and the external surface of the barrel.

Figure 18 shows the probed screw type (90°x5x28 kneading block) and the area under the monitoring. Echo signals reflected respectively from the probe/barrel 'sleeve' interface (L^0) and the barrel 'sleeve'/molten polymer interface (L^1 and L^2) shown in Fig.19 indicate that barrel 'sleeve' thickness hence wear can be monitored. Figure 20 presents the evolutions of echoes reflected from the barrel 'sleeve' internal wall/molten polymer interface L^1 and off the screw (L_{2F}, L_{4F}, L_{6F}, etc.) at the mixing zone from process time 25 s to 27 s. The letters A and B denote the echoes reflected from the different segments of the kneading block illustrated in Fig.18 with the subscripts 1 and 2 representing the contributions from each of the two contributing reflecting surface areas

of each of the denoted segments. From the time delay information, one can see the different barrel/screw clearances for different parts of the bushing. A single trace of signal extracted from Fig. 20 at 26.3 s process time is shown in Fig. 21 and it demonstrates the ability of the clad buffer rod sensor to monitor the screw status.

3.5 Clad Buffer Rod Sensor at the Melting Zone via the Flange

For polymer extrusion and compounding, the conditions of the barrel and screw at the melting zone is also of importance. For the twin-screw extruder used in this investigation, there was a flange at the melting zone and there was no heating band at this location. Commonly the flanges are used on big twin-screw extruders and there is no heating band at these locations. In this section we would like to demonstrate the real-time ultrasonic monitoring at the melting zone via a flange. A clad buffer rod sensor was chosen for illustration purposes although all the above-mentioned sensors could have been used. The schematic diagram and the setup are shown in Fig. 10 and Fig. 22, respectively. The measurement principle is identical to that described in sections 3.3 and 3.4. The probed screw type was a 90°x5x28 and a 45°x5x28 kneading elements as shown in Fig. 23. It is noted that the probed segment B had significant wear.

Figure 24 shows the echo signals reflected respectively from the sensor/barrel interface (L^0) and the barrel/molten polymer interface (L^1) captured with the setup shown in Fig. 22. It illustrates the ability of the clad buffer rod sensor to monitor the barrel thickness hence barrel wear using the time delay between the echoes L^0 and L^1. The evolution of echoes reflected from the barrel internal wall/molten polymer interface L^1 and off the screw (L_{2F} and L_{4F}) at the melting zone from process time 35s to 37s is presented in Fig. 25. The letters A and B denote the echoes reflected from the different segments of the kneading block illustrated in Fig. 23 with the subscripts 1 and 2 representing the contributions from each of the two contributing reflecting surface areas of each of the denoted segments. Note that echo signals reflected from the segment B arrive much later than those from A due to the extra travel distance caused by screw wear. A single trace of signal extracted from Fig. 25 at process time 36.3s is shown in Fig. 26 and it demonstrates the ability of the clad buffer rod sensor to measure the barrel/screw clearance at the melting zone. The poor SNR was due to the fact that at the melting zone the polymer was not melted completely. The unmelted pellets scattered ultrasonic energy in all directions and thus reduced the ultrasonic energy reaching the screw and returning back to the sensor.

3.6. Discussion on the Measurement Speed and Accuracy

For the monitoring of barrel wear (or barrel 'sleeve' wear) and screw status (i.e., wear, misalignment, and deflection), the key parameters to be measured are d_B and d_F. They are basically distance measurements and distance d is equal to the product of ultrasonic velocity v in the material and ultrasonic wave travel time t within the thickness of the material. The barrel is normally made of steel. As described in section 2, the thickness d_B can be obtained from the product of v_{LB} and t_B. v_{LB} is a function of temperature, pressure and composition of the barrel steel. It is noted from Reference [15]

and our unpublished data at IMI that the longitudinal velocity v_{LB} in the barrel steel can be calibrated and is about 6000 m/s. Its change versus temperature is about 1 m/s decrease in sound velocity per 1 °C increase in temperature at temperatures below 400 °C. Note that 400 °C is above the highest barrel temperature (around 350°C) for most polymer extrusion processes. From the reference [16] the time delay decreases by about 1ns per increase of 1000 psi for a 10 mm long steel rod. As mentioned in sections 2 and 3 the time delay t_B can be measured from the time delay differences between two echoes, for example, L^1 and L^2 in Fig.4, L^0 and L^1 in Fig.13, L^0 and L^1 in Fig.19, L^0 and L^1 in Fig.24. Let us assume that the barrel thickness is 100 mm, its composition is uniform, and the barrel temperature and cavity pressure can be measured within an accuracy of ±2°C and ±50 psi, respectively. This corresponds to an uncertainly of time delay of 12 ns. It means that the ambiguity for the absolute barrel wall thickness measurement due to the temperature and pressure measurement uncertainty is 72 μm. Since the SNR of these echoes through proper amplifications is higher than 30 dB, using the commonly practiced cross correlation method [14, 4-7] our previous work reports that the relative measurement accuracy for the time delay t_B in the extrusion conditions that the temperature and pressure are 'stable" is better than 0.5 ns for a steel with a length less than 130 mm [17]. This 0.5 ns leads to an additional uncertainty of ~3 μm in d_B measurement. Furthermore, let 'stable' represent that the temperature and pressure varies within ±0.5°C and ±25 psi, respectively, then the uncertainty for the relative barrel wall thickness measurement is better than 22.5 μm. In addition, due to the high SNR shown in Figs.4, 13, 19 and 24 the monitoring of the barrel wear can be monitored real-time.

For the monitoring of screw status, the barrel/screw clearance d_F should be measured, where $d_F = v_{LP}*t_P$ with v_{LP} being the ultrasonic velocity in the polymer melt. Note that v_{LP} is also a function of temperature and pressure. The accuracy of the screw wear and deflection measurement critically depends on this parameter. v_{LP} can be calibrated under the controlled temperature and pressure using the device developed in [18]. In Reference [19] for the polypropylene (PP) melt the velocity change is about 2m/s per °C and the average velocity is around 1100m/s. In our experience, most polymer melts exhibit the similar rate of change. As far as pressure is concerned the velocity change is about 4.4 m/s per 100 psi for the PP melt [20]. From our experience the velocity change of LDPE and HDPE versus temperature and pressure variation is very similar to that of PP.

Let us assume that for large extruders the gap d_F between the barrel internal wall and the top surface of the screw flight is 1mm, the composition of the polymer melt is uniform, and the melt temperature and melt pressure can be measured within an accuracy of ±5°C and ±100 psi, respectively. This corresponds to an uncertainly of time delay of 24 ns. It means that the ambiguity for the absolute d_F measurement due to the temperature and pressure measurement uncertainty is 27 μm. Since the SNR of these echoes shown in Figs.6, 9, 15, 21 and 26 is not high (<20 dB), using the commonly practiced cross correlation method [14, 4-7] the relative measurement accuracy for the time delay t_P in the extrusion conditions that the temperature and pressure are 'stable" is better than 10 ns. These 10 ns induce an additional uncertainty of 11 μm in d_F measurement. Also let 'stable' represent that the temperature and pressure varies within ±1.0°C and ±50 psi, respectively, then the uncertainty for the relative d_F measurement is better than 18 μm.

Because of the low SNR in the ultrasonic signals shown in Figs.6, 9, 15, 21 and 26 and complex evolution patterns of reflected echoes, there could be need for rather dedicated signal processing techniques for real-time and automatic determination and display of screw status. However, for extruder and process diagnostic purposes, it is usually not a practical limitation to allow seconds or even minutes for the display of screw status. Under this circumstance, the images shown in Figs.5, 14, 20 and 25 together with automatic pattern recognition methods can be used for the calculation of d_F and then a much improved accuracy is expected. With the help of these images, even with naked eye one may be able to pinpoint most abnormalities of an extruder or a process. By installing and using multiple ultrasonic sensors along the extruder barrels, the screw misalignment and deflection profile could be determined and an improved accuracy on screw wear measurement can be expected. It is also noted that for large extruders the surface of the tip of a screw flight is much larger than those of the screws used in this study. Thus, a much stronger ultrasonic echo strength, and as a consequence, a much larger SNR, are expected. As mentioned earlier, a high SNR can certainly reduce uncertainty in the time delay measurement.

4. Conclusions

Ultrasonic sensors together with a fast data acquisition system have been used to perform in-line measurements of barrel wear and screw status during low-density polyethylene and high-density polyethylene extrusions on a W&P 30 mm twin-screw extruder. A sol-gel sprayed piezoelectric thick BIT/PZT film high temperature (HT) ultrasonic transducer (UT) was evaluated at the pumping zone, a stand-alone HTUT at the pumping zone, an air-cooled buffer rod sensor consisting of a room temperature UT and a non-clad buffer at the mixing zone, and air-cooled buffer rod sensors consisting of a room temperature UT and a clad buffer rod at the mixing zone and at the melting zone via a flange. The application of these sensors is non-intrusive and non-destructive, and the measurement can be performed in real-time. The tradeoffs of these sensors have been presented. The measurement speed and accuracy have been discussed. This investigation has successfully demonstrated the ability of ultrasound for in-line barrel wear and screw status monitoring.

Acknowledgements

The authors are grateful to C. Corbeil, H. Hébert and J. Tatibouët for their technical assistance. The work was supported in part by the NRC-NSC, Taiwan project and the Natural Sciences and Engineering Research Council of Canada.

Reference

[1] S.H. Collins, *Plastics Compounding*, May/June, 113 (1982).

[2] L.S. Steward, *Plastics Engineering*, 53 Jan. (1985).

[3] E. Steward, *American Kuhne*, Tech Tip no.1, March 1 (2003).

[4] L. Piché, *Polymer Eng. Sci*., **24**, 1354 (1984).

[5] L. Piché, A. Hamel, R.Gendron, M.M.Dumoulin and J. Tatibouët, US Patent, no.5,433,112, July 18, 1995.

[6] J . Tatibouët and M.A. Huneault, Inter. Polymer Processing, **17**, 49 (2002).

[7] Z. Sun, C.-K. Jen, C.-K. Shih and D. Denelsbeck, Polymer Eng. Sci., **43**, 102 (2003).

[8] D. Barrow, T.E. Petroff, R.P. Tandon, M. Sayer, *J. Apply. Phys.*, **81**, 876 (1997).

[9] M. Kobayashi, T.R. Olding, M. Sayer, and C.-K. Jen, *Ultrasonics*, **39**, 675 (2002).

[10] M. Kobayashi, C.-K. Jen, C. Corbeil, Y. Ono, H. Hebert and A. Derdouri, to appear in Proc. IEEE Ultrasonics Symp., Honolulu, Hawaii, Oct.5-8, 2003.

[11] H. Mrasek, D. Gohlke, K. Matthies and E. Neumann, *NDTnet*, **1** Sept. 1 (1996).

[12] C.-K. Jen, L. Piche and J.F. Bussiere, *J. Acoust. Soc. Am*., **88**, 23 (1990).

[13] C.-K. Jen, J.-G. Legoux and L. Parent, *NDT&E Int'l*, **33**, 145 (2000).

[14] D. Ramos França, C.-K. Jen, K.T. Nguyen and R. Gendron, *Polymer Eng. Sci*., **40**, 82 (2000).

[15] C.B. Scruby and B.C. Moss, *NDT&E Int'l*, **26**, 177 (1993).

[16] T.F. Chen, K.T. Nguyen, D. Ramos-França, C.-K. Jen, I. Ihara and J. TatbouëT, Proc. QNDE Conf., **19B**, 2021 (1999).

[17] T.-F. Chen, K.T. Nguyen, S.-S. L. Wen and C.-K. Jen, *Measurement Sci. and Technology*, **10**, 139 (1999).

[18] L. Piché, F. Massines, A. Hamel and C. Neron, *US Patent* no.4,754,645, July 5, 1988.

[19] L. Piché, F. Massines, G. Lessard and A. Hamel, *Proc. IEEE Ultrasonics Symp*., 1125 (1987).

[20] L. Piché, D. Lévesque, R.Gendron and J. Tatibouët, Proc. VIth Symp. on Non Destructive Characterization of Materials, 37 (1993).

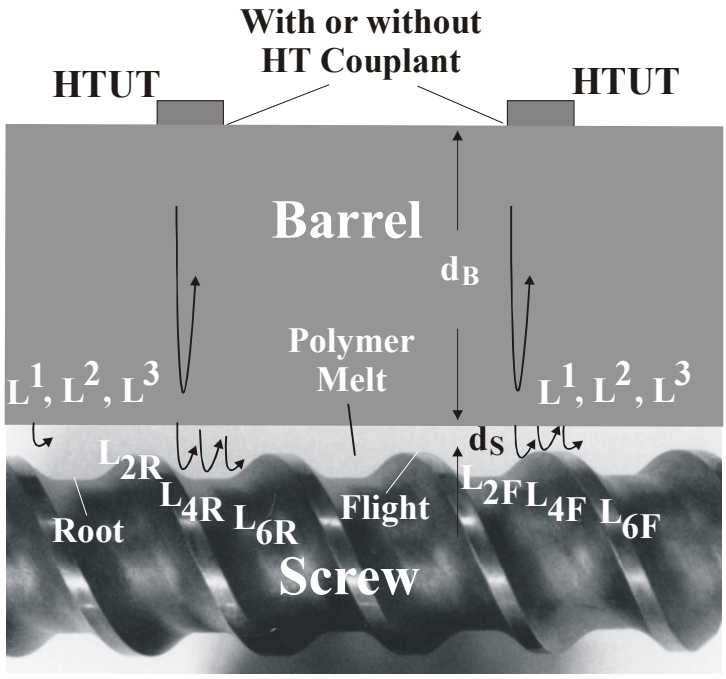

Fig. 1. A schematic diagram of the ultrasonic waves propagating in the extruder barrel and polymer melt.

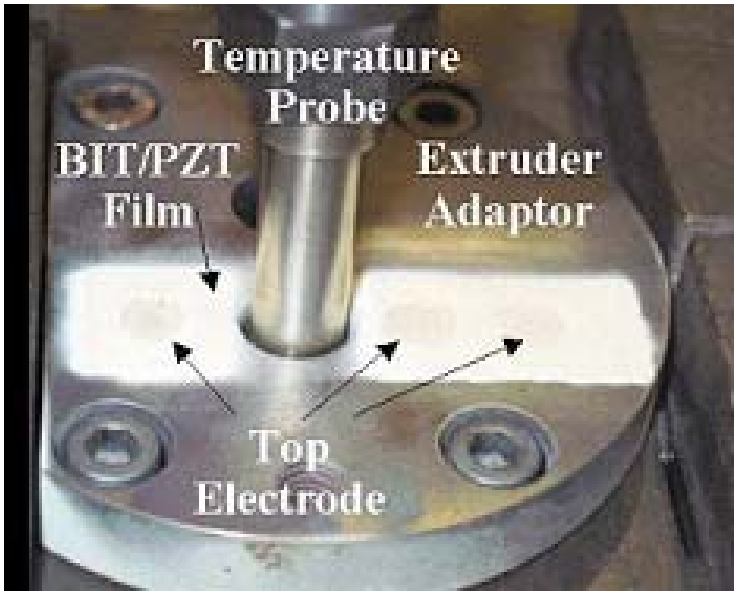

Fig. 2. Sol-gel sprayed BIT/PZT HTUTs deposited onto the top external surface of an extruder adaptor placed at the pumping zone of the extruder.

Fig. 3. The type and area of the screw under the monitoring at the pumping zone with the center HTUT shown in Fig. 2.

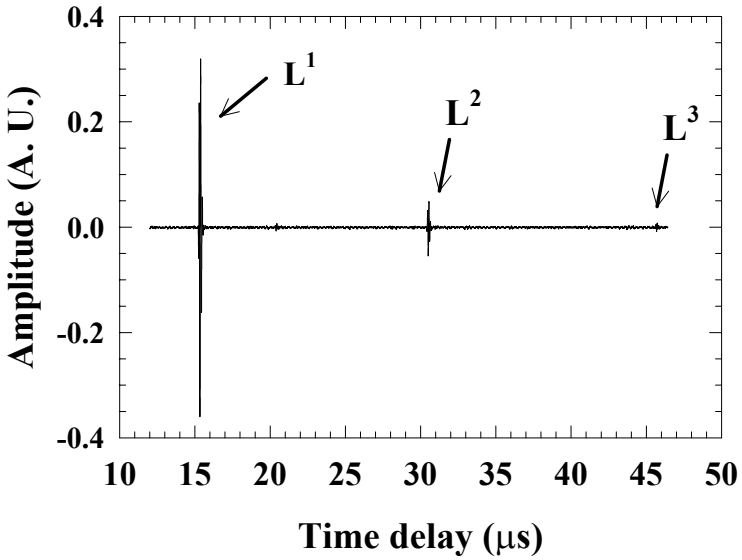

Fig. 4. Echoes reflected at the adaptor/molten polymer interface and received by the sol-gel sprayed HTUT shown in the center of Fig.2.

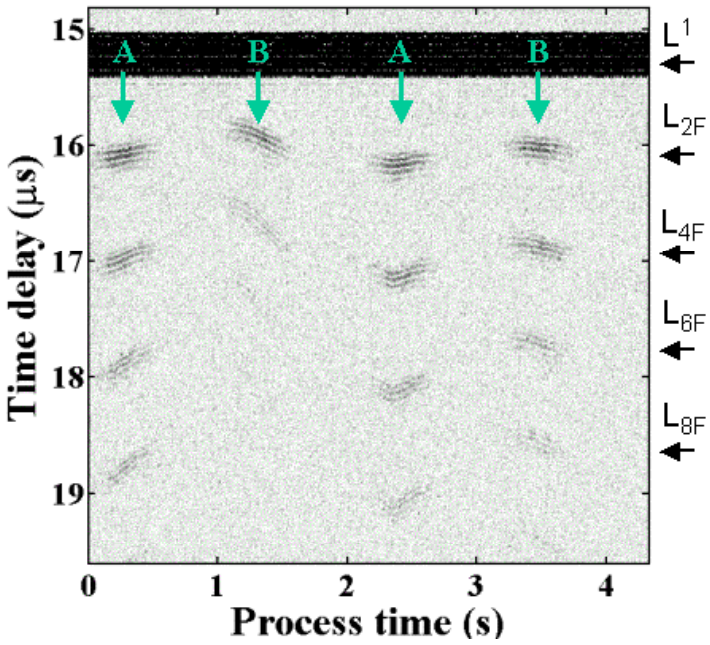
A
B
A
B
L1
L2F
L4F
L6F
L8F
Time delay (µs)
15
16
17
18
19
0
1
2
3
4
Process time (s)

5(a)

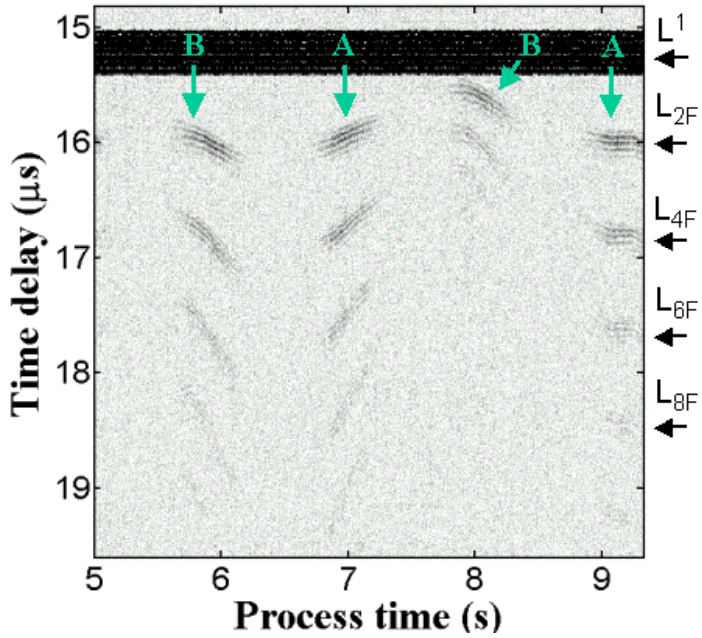
B
A
B
A
L1
L2F
L4F
L6F
L8F
Time delay (µs)
15
16
17
18
19
5
6
7
8
9
Process time (s)

5(b)

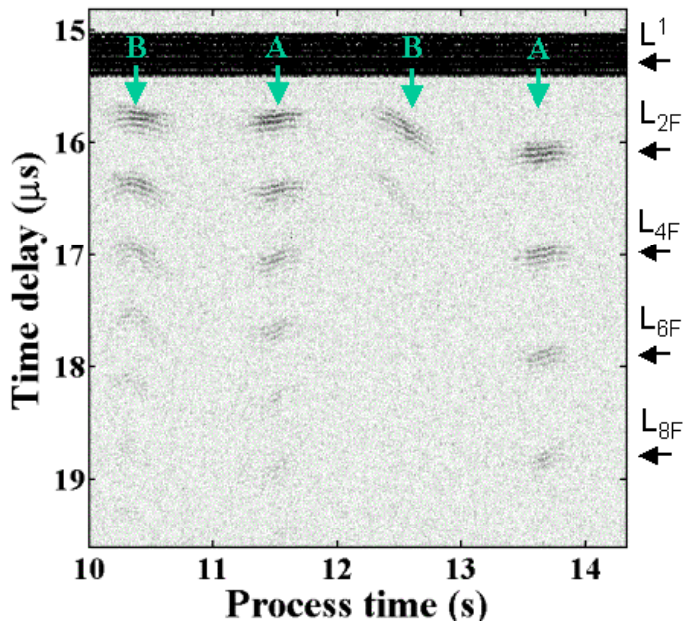

5(c)

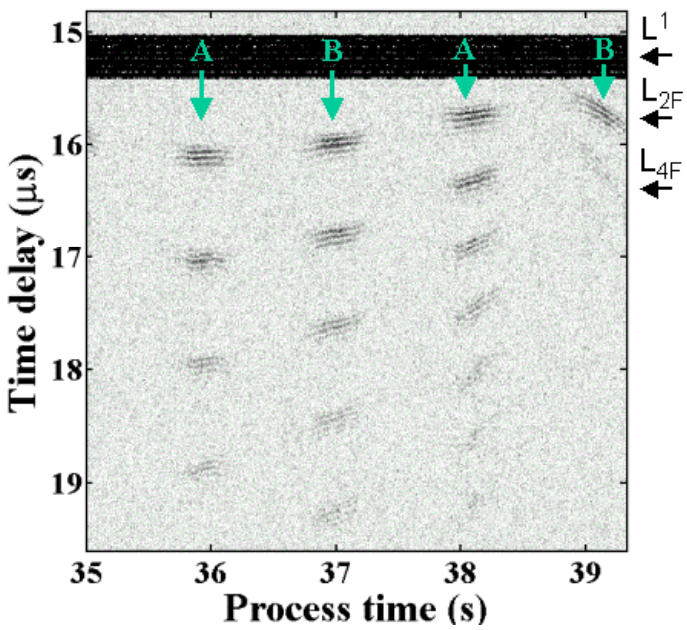

5(d)

Fig. 5. Evolution of echoes reflected at the adaptor/molten polymer interface (L^1) and off the screw flight (L_{2F}, L_{4F}, and L_{6F}, etc.) received at the pumping zone with the sol-gel sprayed HTUT during the first 40s into the data acquisition. The letters A and B denote the echoes reflected by the tip of each of the two screw flights within one revolution.

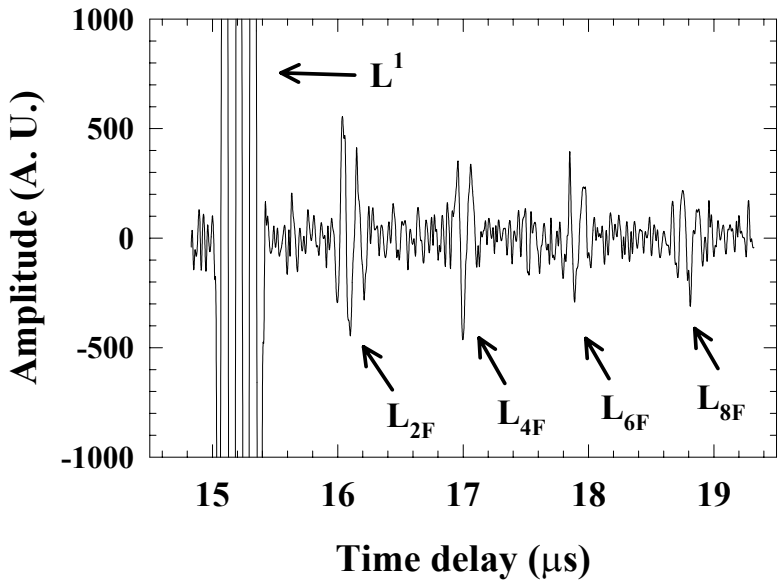

Fig. 6. A single trace of signal extracted from Figure 5(a) at 0.25s process time.

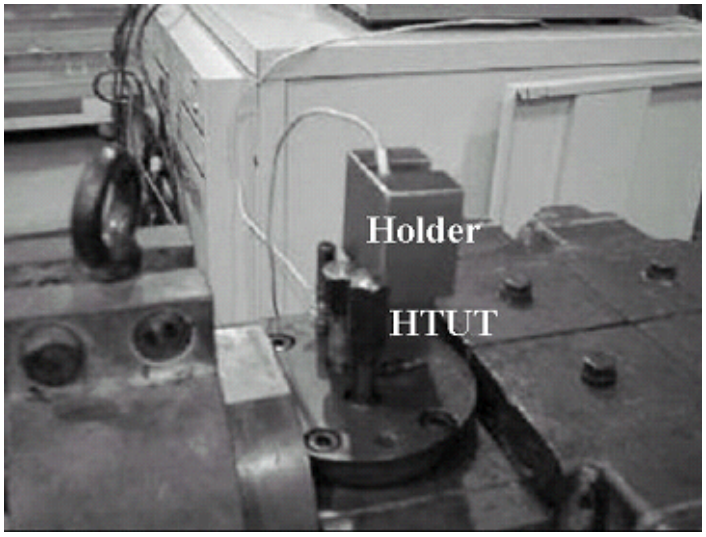

Fig. 7. Stand-alone high temperature UT with a holder placed at the top of the extrusion adaptor and aligned with the screw underneath.

Fig. 8. The screw bushings (28/28 RH) probed in setup of Figure 7.

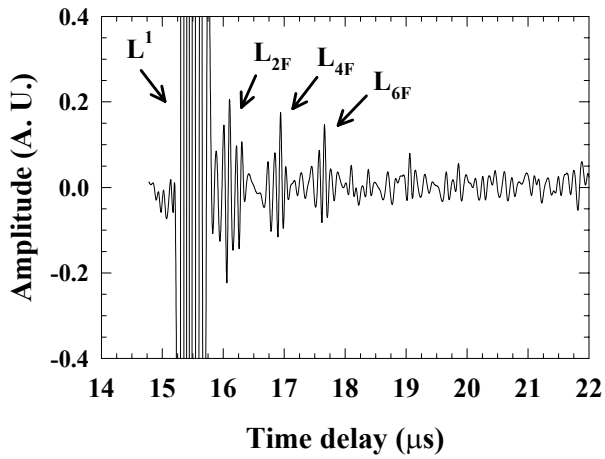

9(a)

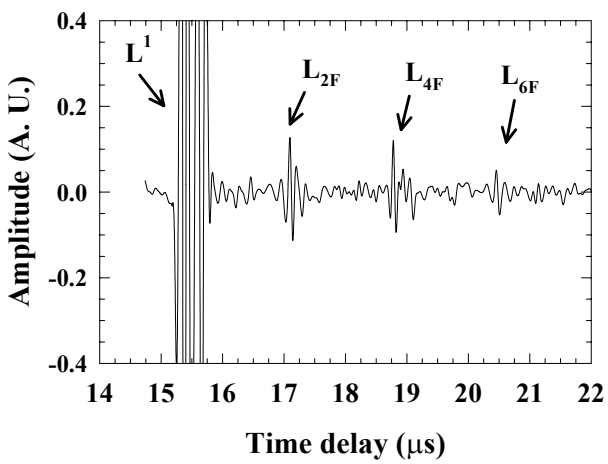

9(b)

Fig. 9. Echoes reflected at the adaptor/molten polymer interface (L^1) and off the un-worn and the simulated worn (downsized) screws (L_{2F}, L_{4F}, and L_{6F}) at the pumping zone.

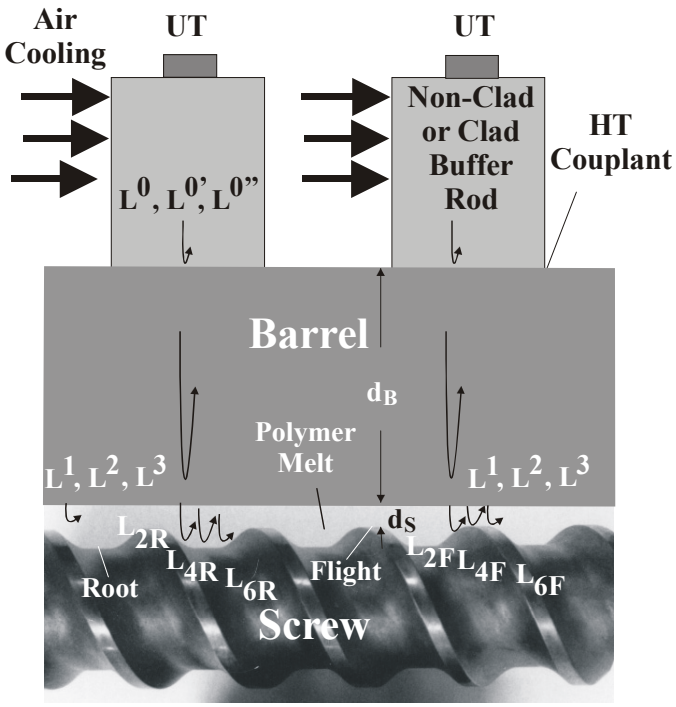

Fig. 10. Schematic diagram of the ultrasonic waves propagating in the buffer rod, extruder barrel and polymer melt.

Fig. 11. A non-clad buffer rod probe mounted at the bottom of a barrel at the mixing zone with the help of a holder. The heating band did not cover the bottom surface of the barrel.

Fig. 12. The probed screw type and area under the monitoring of the probe shown in Fig. 11 at the mixing zone.

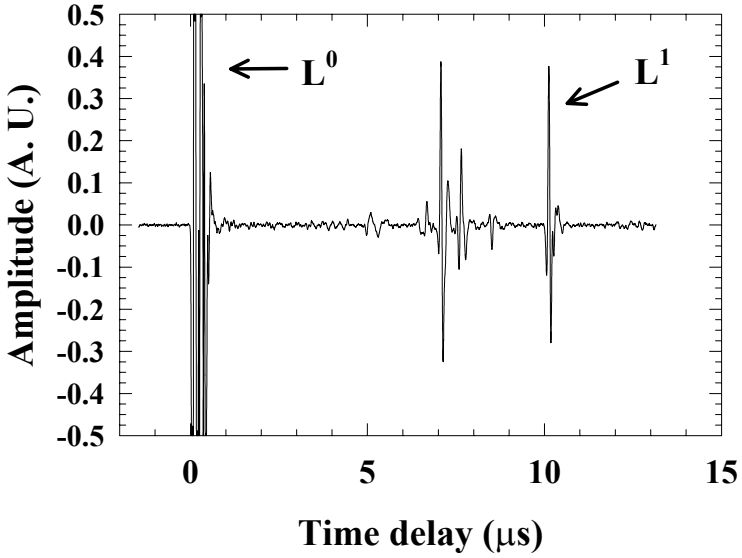

Fig. 13. Echo signals reflected respectively from the probe/barrel interface (L^0) and the barrel/molten polymer interface (L^1) captured with the setup shown in Fig. 11.

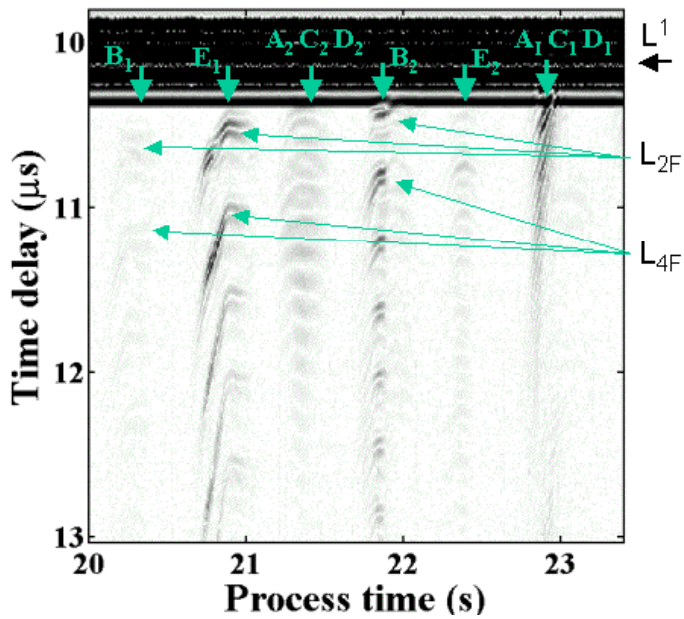

Fig. 14. Evolution of echoes reflected from the barrel internal wall/molten polymer interface L^1 and off the screw (L_{2F}, L_{4F}) at the mixing zone. The letters A, B, C, D, and E denote the echoes reflected from the different segments of the kneading blocks illustrated in Fig.12 with the subscripts 1 and 2 representing the contributions from each of the two contributing reflecting surface areas of each of the denoted segments.

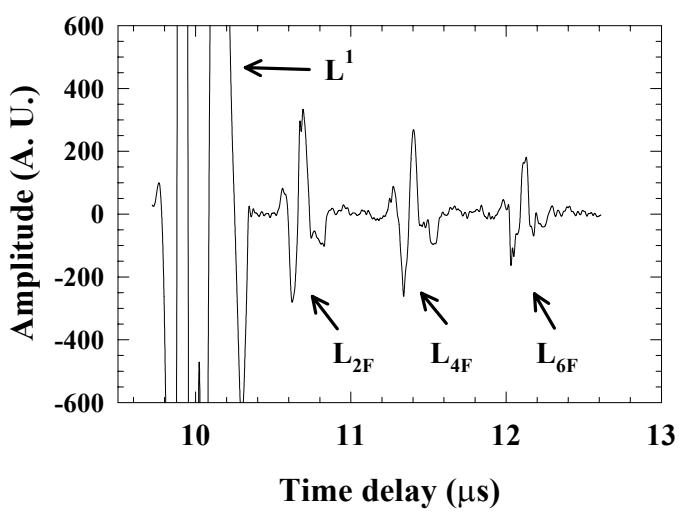

Fig. 15. A single trace of signal extracted from Fig. 14 at 20.75s process time.

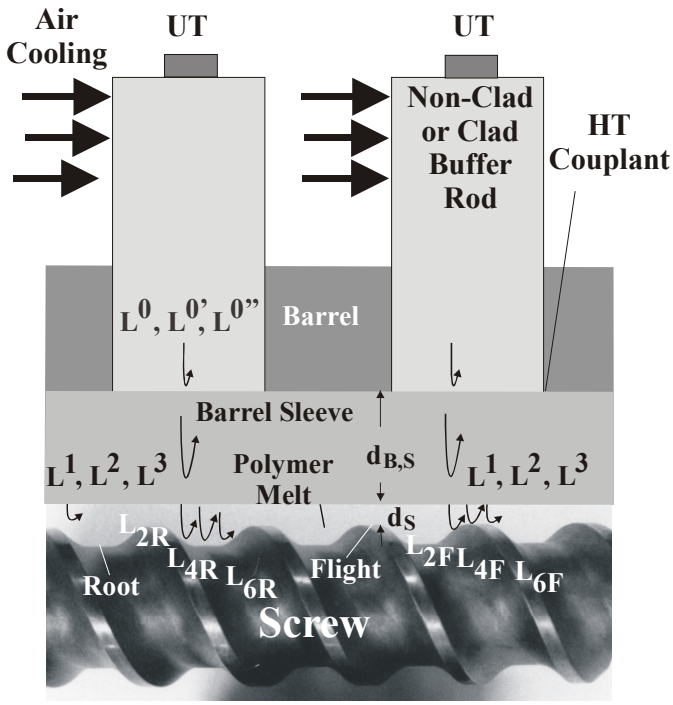

Fig. 16. Schematic diagram of the ultrasonic waves propagating in the buffer rod, extruder barrel sleeve and polymer melt.

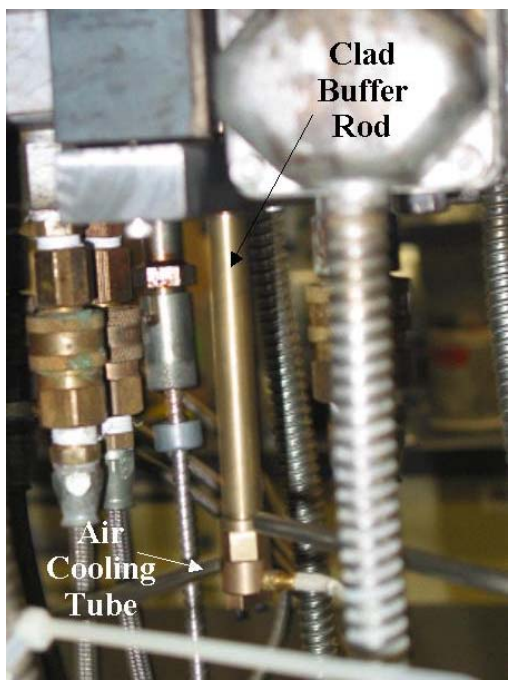

Fig. 17. A clad buffer rod probe mounted at the bottom of a barrel at the mixing zone with the help of a holder. The heating band did not cover the bottom surface of the barrel.

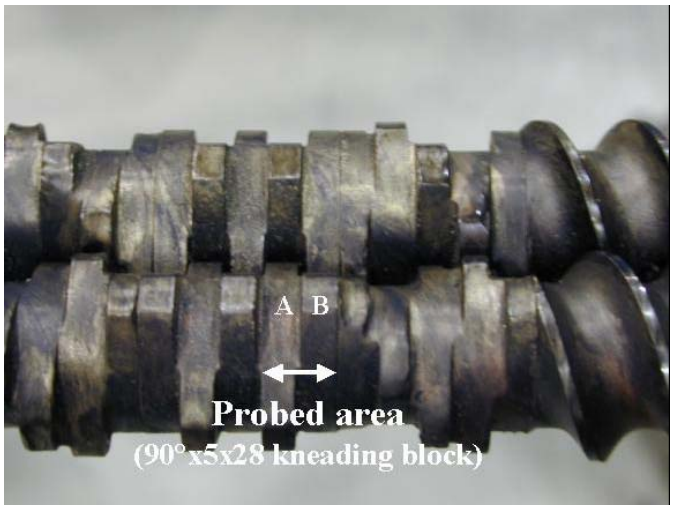

Fig. 18. The probed screw type and area under the monitoring of the clad buffer rod probe shown in Fig.17.

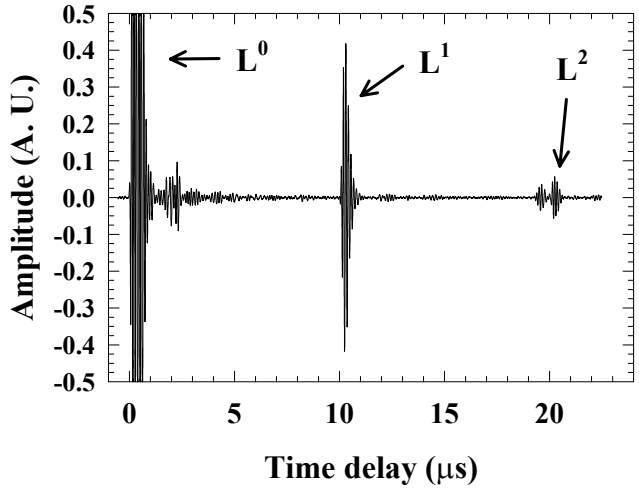

Fig. 19. Echo signals reflected respectively from the probe/barrel 'sleeve' interface (L^0) and the barrel 'sleeve'/molten polymer interface (L^1 and L^2) captured with the setup shown in Fig.17.

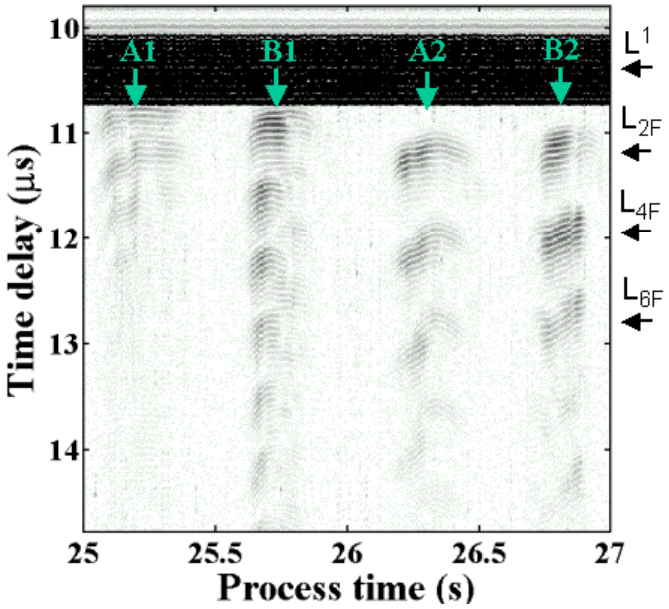

Fig. 20. Evolution of echoes reflected from the barrel sleeve internal wall/molten polymer interface L^1 and off the screw (L_{2F}, L_{4F}, L_{6F}, etc.) at the mixing zone. The letters A and B denote the echoes reflected from the different segments of the kneading block illustrated in Fig.18 with the subscripts 1 and 2 representing the contributions from each of the two contributing reflecting surface areas of each of the denoted segments.

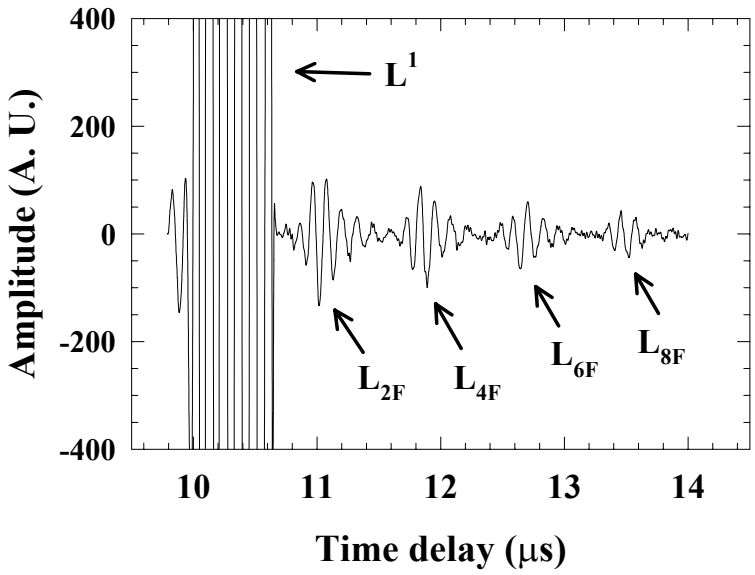

Fig. 21. A single trace of signal extracted from Fig. 20 at 26.3s process time.

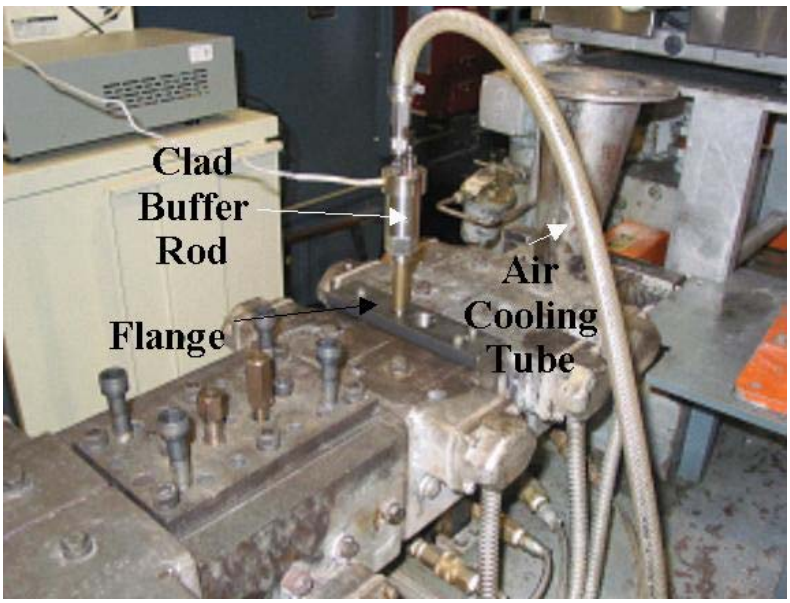

Fig. 22. A clad buffer rod probe mounted at the top of a flange at the melting zone with the help of a holder.

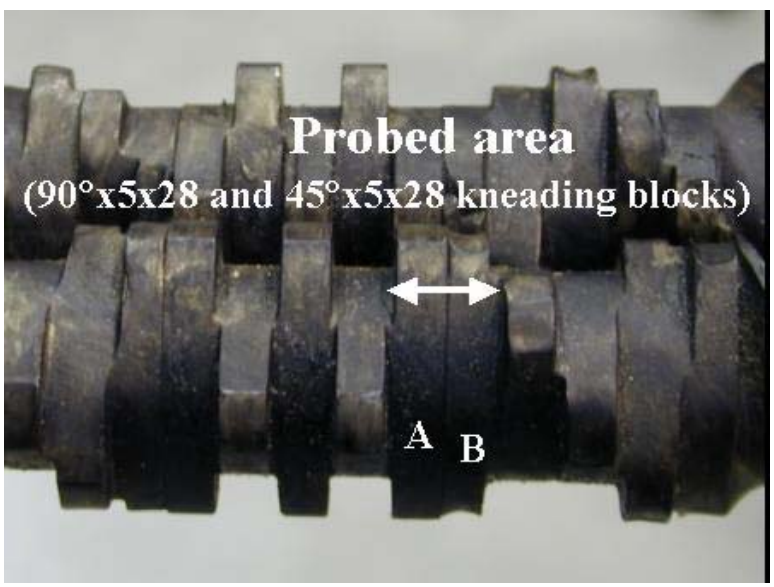

Fig. 23. The probed screw type and area under the monitoring of the probe shown in Fig. 21. Note that the probed segment B has significant wear.

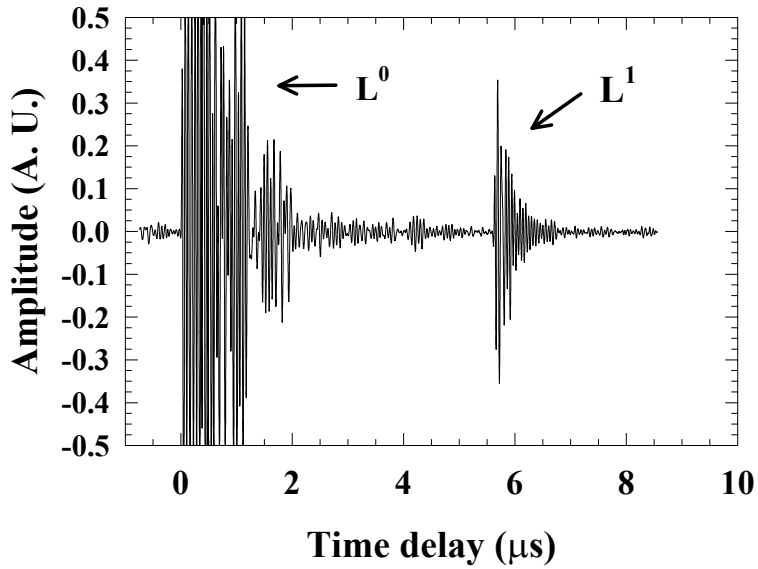

Fig. 24. Echo signals reflected respectively from the probe/barrel interface (L^0) and the barrel/molten polymer interface (L^1) captured with the setup shown in Fig. 22.

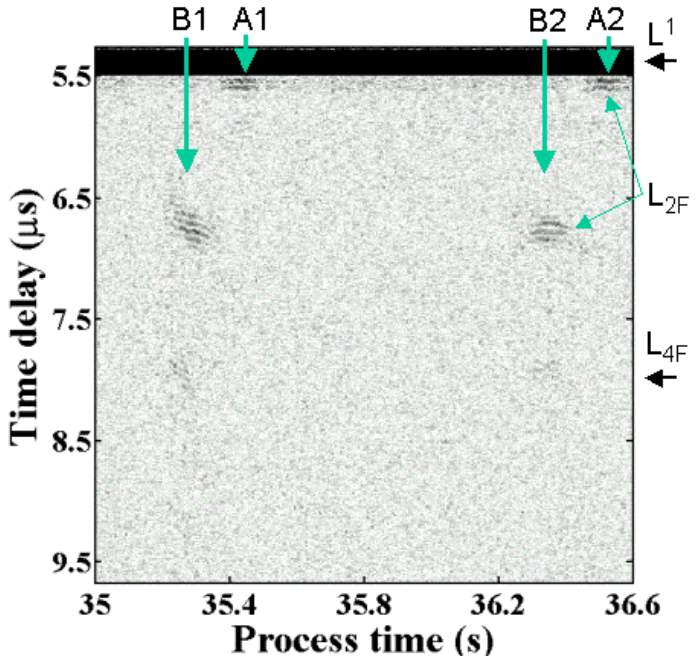

Fig. 25. Evolution of echoes reflected from the barrel internal wall/molten polymer interface L^1 and off the screw (L_{2F} and L_{4F}) at the melting zone. The letters A and B denote the echoes reflected from the different segments of the kneading block illustrated in Fig.23 with the subscripts 1 and 2 representing the contributions from each of the two contributing reflecting surface areas of each of the denoted segments. Note that echo signals reflected from the segment B arrive much later than those from A due to the extra travel distance caused by screw wear.

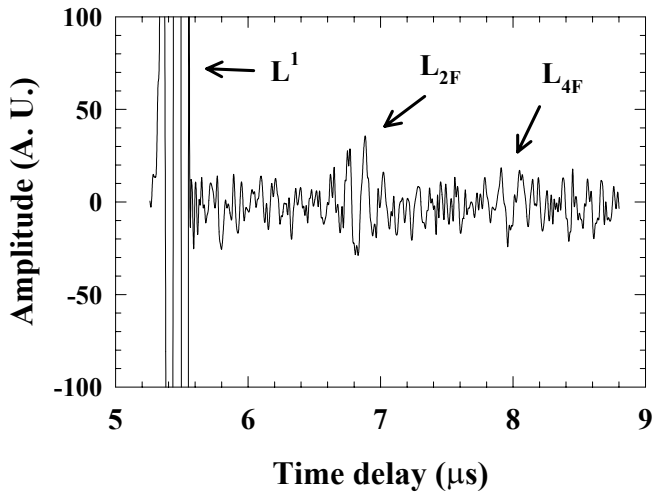

Fig. 26. A single trace of signal extracted from Fig. 25 at 36.3s process time.